Free-surface microfluidics: exploring new actuation and sensing methods

Gan Yu, Nan Lei, Xiaolin Chen, Wei Xue and Jie Xu*

Mechanical Engineering, Washington State University, Vancouver, WA 98686, USA
jie.xu@wsu.edu

ABSTRACT

In this paper, we present recent advancements in our group on the development of acoustic actuation and electrochemical sensing technologies that can be used for future free-surface microfluidics. We first show that actuation in free-surface microfluidics can be achieved by acoustic radiation forces. Due to the fact that air and water have very different acoustic impedances, the free surfaces act as perfect sound reflectors. The shape of the free surfaces is important in controlling the acoustic radiation forces. We developed two techniques to precisely control the free-surface shapes: edge pinning and biphilic pinning. We also show that electrochemical sensing inside a free-surface droplet can be achieved by a simple graphene sensor fabricated with a mask-free process using focused ion beam. The experiment shows that the resistance of the sensor decreases linearly with increasing pH values in the free-surface droplets. The novel actuation and sensing methods developed here can be promising candidates for future free-surface microfluidics.

Keywords: actuation, sensing, acoustic radiation force, graphene, focused ions beam

1 INTRODUCTION

Unlike traditional microchannel-based microfluidics, free-surface microfluidics features no channel, ease to clean, simple design, fabrication and operation, as well as external access to the samples. It has been widely studied that free-surface droplets can be actuated and manipulated by Electrowetting-on-dielectric (EWOD) technology [1]. However, little has been done to study the actuation and sensing inside free-surface droplets, which are important components for future development of free-surface microfluidic systems. In this paper, we explore an actuation method using acoustic radiation force and a sensing method using a graphene device, both can be used in future free-surface microfluidics.

2 ACOUSTIC ACTUATION

Actuation in free-surface microfluidic devices is needed to achieve important lab-on-a-chip tasks, such as particle manipulation, trapping, and transporting. It has been found that acoustic radiation force in an ultrasound field can be used for actuation, a technology termed as acoustophoresis. As an emerging and promising actuation tool [2], acoustophoresis has many advantages over other methods: it is a non-contact and non-invasive method, and it can work with almost any type of microscale particles regardless of their optical, magnetic or electrical properties. In this paper, we develop novel acoustophoresis techniques for particle manipulation in various shapes of free-surface droplets, where the acoustic standing wave field and field-induced radiation force can be precisely controlled.

2.1 Acoustic Radiation Force

Droplet with water/air interface serves as an excellent acoustic resonator in our experiment. According to the theory developed in [2], when an acoustic wave travels from water into air, most acoustic waves will be reflected back, because of the high acoustic impedance ratio. The reflected acoustic wave inside a free-surface droplet can form standing waves, which will exhibit acoustic radiation force. Acoustic radiation force is a non-linear acoustic effect that can be used to attract particles to either the nodes or anti-nodes of the standing wave depending on the acoustic contrast factor ϕ:

$$\phi(\beta,\rho) = \frac{5\rho_p - 2\rho_m}{2\rho_p + \rho_m} - \frac{\beta_p}{\beta_m} \quad (1)$$

which depends on the the densities and compressibilities of the particle (ρ_p, β_p) and the medium (ρ_m, β_m).

2.2 Experimental Setup and Shape Control

Acoustic standing wave inside a free-surface droplet are generated with a piezoelectric actuator attached to an aluminum substrate, as shwon in Figure 1.

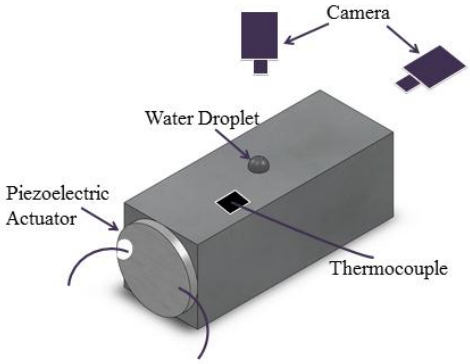

Figure 1: The experimental system used for acoustic actuation inside free-surface droplets.

The standing wave pattern is defined by both frequency and the shape of the free-surface droplets. In our experiments, we developed two techniques for the shape control as shown in Figure 2.

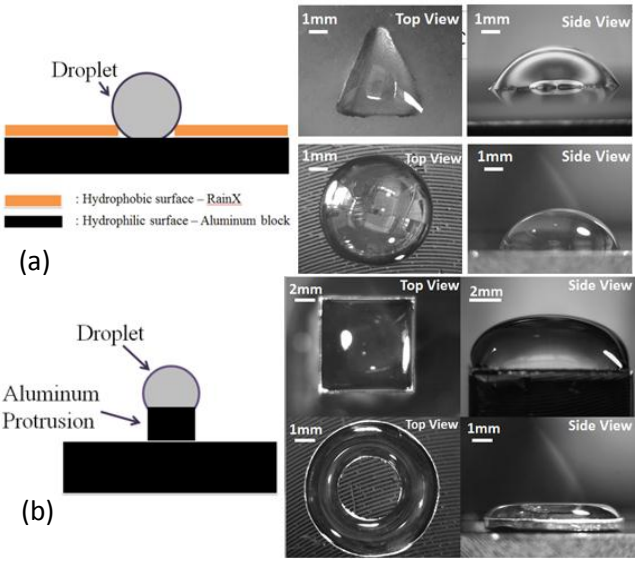

Figure 2: Techniques for droplet shape control. (a) biphilic pinnin; (b) edge pinning.

The first method is biphilic pinning, which is achieved by coating hydrophilic aluminum with hydrophobic patterns using RainX solution. Different shapes of masks are used during coating, so that various biphilic patterns can be created. If a small amount of water is placed onto the pattern, the droplet will tend to stay in the hydrophilic areas. Using this method, circular and triangular droplets are created as demonstrated in Figure 2(a). The second method is edge pinning, which is achieved by adding protrusions on top of the aluminum surface. Various base shapes are used, and their edges can be used to pin the free surface of the droplet. Using this method, rectangular and annular droplets are created as demonstrated in Figure 2(b).

2.3 Experimental Results and Simulations

After the piezoelectric actuator is turned on, an acoustic field will form inside the droplets. At resonant frequencies, standing wave will form and particles (Copolymer Microsphere Suspension 11 μm, Thermo Scientific) inside the droplets will be actuated by the acoustic radiation force. The movement of the particles will form in the end different patterns under different frequencies. In the experiments, these patterns were recorded by the camera and simulation results were conducted using ANSYS® software. In the ANSYS simulation, a 2-D acoustic element type Fluid29 was employed for acoustic modal analysis of the pressure field in the simplified droplet chambers. An impedance boundary condition was specified at each air/water interface. To ensure result convergence, the mesh densities of the models were increased as frequency goes up to have at least 5 elements per wavelength.

Figure 3 reports typical experimental and numerical results. The white lines in the experimental results are accumulated particles in the acoustic field. The The green areas in the numerical results represent the pressure nodal zones where pressure oscillation is zero, and the blue/red areas represent the anti-nodal zones where pressure oscillation is maximal. The simulated patterns show good consistency with experimental results and prove that the locations where particles gather in the experiments correspond to the nodal zones in the ANSYS results. Similar phenomena can also be observed in variously shaped free-surface droplets.

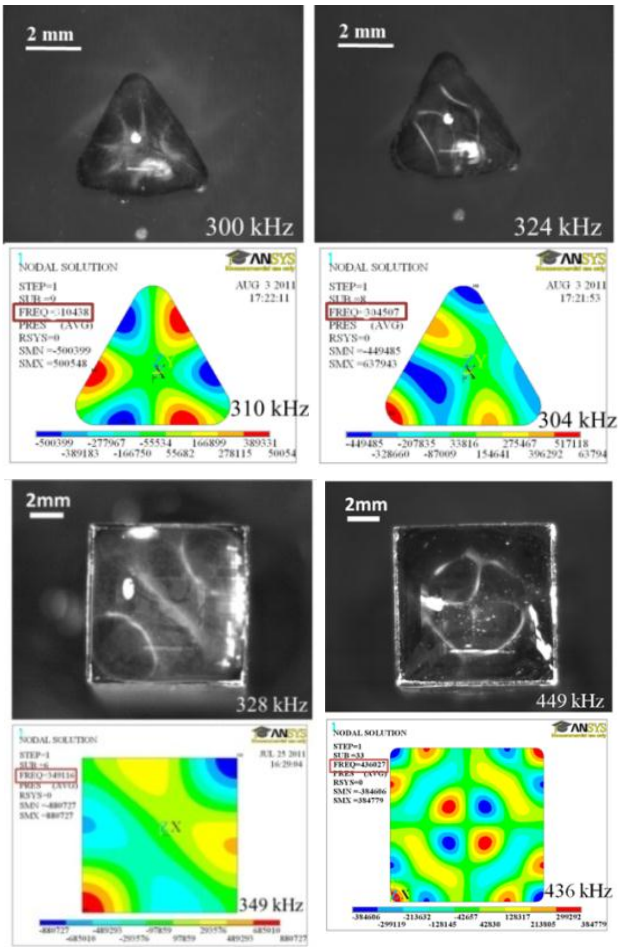

Figure 3: Acoustic manipulation of micrometer sized particles inside free-surface droplets. The pattern of particles is affected by the free surface shape as well as the acoustic frequency. The experimental results matches simulation results well.

3 ELECTROCHEMICAL SENSING

The ability to precisely detect chemical and biological species inside free-surface microfluidics is extremely important in many applications, such as genomics, clinical

diagnosis and pharmaceutics. Traditional optical detection methods require very complex techniques and labeling processes. Alternatively, the electrical detection methods using novel nanomaterial devices have been extensively studied in the past decade [4, 5]. As one of the most promising material, graphene has unique electronic structures: single atom thickness with the π states (valance band) and π* states (conduction band) touching at the Dirac points [6]. The symmetric band structure of graphene makes it directly amenable to chemical and physical modification. In addition, the high carrier mobility of graphene makes the modification detectable by simply monitoring its conductivity change [7]. Since the discovery of graphene [8], there is great potential for building graphene-based high-sensitivity, label-free, miniaturized electrostatic or electrochemical sensors [9].

One of the key challenges in current research and development of graphene-based sensors is material handling and device fabrication [10]. Conventional microfabrication approaches, such as lithography and etching, often require multiple complex steps including masking and aligning. Also graphene is often configured as the semiconducting material in transistors, which require the fabrication of a gate. In this paper, we report a simplified graphene device where the graphene is configured as a planar chemiresistor. The manufacture of this device consists of a mask-free focused ion beam (FIB) process and several easy post-processing steps that can be done manually. In the end, we demonstrate the ability of this device in monitoring pH values in free-surface droplets. As a new material, the application of graphene is still at the infant stage, and the performance of our graphene-based devices cannot yet compete against current commercial devices. However, the miniaturized size, low cost and the integration ability make graphene-based sensors more suitable for future free-surface systems.

3.1 Materials and Methods

Figure 4 sketches the entire mask-free fabrication process of our graphene sensor. Graphene sheets were first made by mechanical exfoliation of bulk graphite (Kish Graphite, purchased from Graphene Supermarket) with scotch tape and randomly deposited onto a 285 nm SiO2 layer on a silicon wafer (P/B(100), 1-10 ohm-cm purchased fromuniversitywafer.com). An optical microscope and a camera (Nikon MM-40 and DXM 1200) were then used to identify and locate individual graphene sheets (as sketched in Figure 4a). This is currently the easiest and most popular way to spot graphene crystallites among copious thicker flakes. Usually, a few micron-sized graphene can be found over a millimeter-sized area, which is already sufficient for our purpose. A dual beam system (FEI Quanta 3D 200i) was used for the fabrication of electrodes and observation of the sample: an ion beam for electrode deposition and an electron beam for imaging. The area of interest on the sample was positioned at the eucentric point where the two beams cross. At this location, the electron beam could provide in situ imagining of the graphene. The FIB employs highly-focused Pt+ ion beam scanned over the desired areas of the sample surface for electrode deposition with approximately 20 nm precision. To expand the contact platinum electrodes, two millimeter sized testing pads, as sketched in Figure 4c, were conveniently made by carefully painting a layer of silver on the wafer using high-purity conductive silver paint (SPI 05001-AB), operated under a stereo microscope (Nikon S2800). To eliminate the potential contamination of silver particles from dissipating into the testing samples, a layer of polydimethylsiloxane (PDMS) (Dow Corning Sylgard 184) was carefully cured on top of the silver electrodes and leaves a 200-300μm gap large enough for future droplet deposition on the graphene sheet. The configuration of a fabricated graphene device is sketched in Figure 4d. In the end, an annealing step was used to help improve the electrical interconnection.

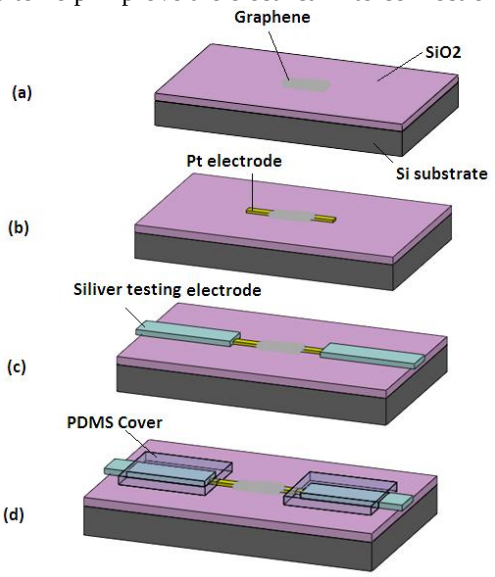

Figure 4: The mask-free fabrication process of a graphene sensor for free-surface microfluidics.

3.2 Experiment and Results

To demonstrate the graphene device as a pH sensor for free-surface microfluidics, droplets with different pH values were directly deposited on top the graphen device. In the experiment, the resistance of the device under a constant current were monitored and recorded in real time by a semiconductor analyzer (Agilent Technologies B1500A). After the resistance of the device in the air was stabilized, the first pH buffer drop was carefully placed on top of the graphene sheet as shown in Figure 5. After approximately 1~2 minutes when the resistance became stable, this pH buffer drop was carefully sucked up by vacuum, and then more buffer drops with different pH values were applied and removed repeatedly in the same way. In our experiments, buffers with pH values from 4 to 10 (standard buffer solutions from Fisher Scientific) were tested.

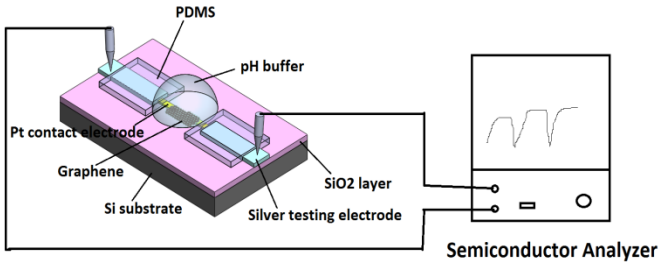

Figure 5: Experimental system for pH sensing in free-surface microfluidics using graphene as an electrochemical sensor.

Figure 6(a) reports a real time measurement of the resistance of our graphene device under a constant current at 10 μA. The resistance of the device in the air is approximately 86 kΩ. When a drop of pH-4 buffer was placed on the graphene, the resistance rapidly decreased to 59.2 kΩ. The resistance is then decreased by 2.2 kΩ when pH-5 buffer was placed on the graphene. Similar amount of decrement is observed when the pH buffer was changed to pH-6, Ph-7, pH-8, pH-9 and pH-10.

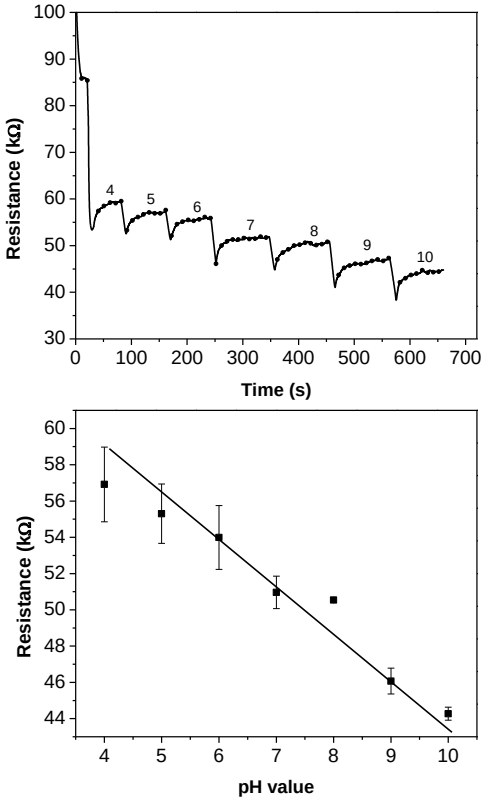

Figure 6: (a) Real-time resistance measurements of the graphene sensor when exposed to pH buffers from pH-4 to pH-10; (b) complied resistance data from multiple measurements plotted as a function of pH values.

Figure 6(b) shows the average values (dots) and standard deviations (error bars) of the resistance from multiple measurements on this specific device. A linear correlation can be used to describe the curve in Figure 5b: $R = (-2.13 \times pH + 66.11)$ kΩ. This equation indicates that the sensitivity of the particular device is 2.13 kΩ/pH.

4 CONCLUSION

In this paper, we explored new actuation and sensing methods for free surface microfluidics. Specifically, acoustic actuation and electrochemical sensing technologies have been developed and demonstrated in free surface microfluidics. We show that acoustic radiation force controlled by free-surface shape and acoustic frequeny can be used to actuate particles. We also show that a simple graphene device fabricated with a mask-free process using focused ion beam can be used for electrochemical sensing inside a free-surface droplet. The novel actuation and sensing methods developed here can be promising candidates for future free-surface microfluidics.

5 ACNOWLEDGEMENTS

We thank the financial support from DARPA Young Faculty Award: N66001-11-1-4127.

REFERENCES

[1] Wheeler, A.R., Science, 2008. 322(5901): p. 539-540.
[2] S. Oberti, A. Neild, R. Quach and J. Dual, Ultrasonics, 2009, 49, 47-52.
[3] H. Bruus, Theoretical Microfludics, Oxford University Press, 2007.
[4] Cui, Y., Q. Wei, H. Park, and C.M. Lieber, Science, 2001. 293(5533): p. 1289-1292.
[5] Zheng, G., F. Patolsky, Y. Cui, W.U. Wang, and C.M. Lieber, Nature Biotechnology, 2005. 23(10): p. 1294-1301.
[6] Novoselov, K.S., A.K. Geim, S.V. Morozov, D. Jiang, M.I. Katsnelson, I.V. Grigorieva, S.V. Dubonos, and A.A. Firsov, Nature, 2005. 438(7065): p. 197-200
[7] Elias, D.C., R.R. Nair, T.M.G. Mohiuddin, S.V. Morozov, P. Blake, M.P. Halsall, A.C. Ferrari, D.W. Boukhvalov, M.I. Katsnelson, A.K. Geim, and K.S. Novoselov, Science, 2009. 323(5914): p. 610-613
[8] Novoselov, K.S., A.K. Geim, S.V. Morozov, D. Jiang, Y. Zhang, S.V. Dubonos, I.V. Grigorieva, and A.A. Firsov, Science, 2004. 306(5696): p. 666-669.
[9] Geim, A.K. and K.S. Novoselov, Nature Materials, 2007. 6(3): p. 183-191.
[10] Yang, W.R., K.R. Ratinac, S.P. Ringer, P. Thordarson, J.J. Gooding, and F. Braet, Angewandte Chemie-International Edition, 2010. 49(12): p. 2114-2138.